Supplementary Information

A water-soluble DsbB variant that catalyzes disulfide bond formation *in vivo*

Dario Mizrachi[1], Michael-Paul Robinson[1], Guoping Ren[2], Na Ke[2], Mehmet Berkmen[2], and Matthew P. DeLisa[1*]

[1]School of Chemical and Biomolecular Engineering, Cornell University, Ithaca, NY 14853 USA and [2]New England Biolabs, 240 County Rd, Ipswich, MA, 01938, USA

[*]Address correspondence to: Matthew P. DeLisa, School of Chemical and Biomolecular Engineering, Cornell University, Ithaca, NY 14853. Tel: 607-254-8560; Fax: 607-255-9166; Email: md255@cornell.edu

Supplementary Results

a

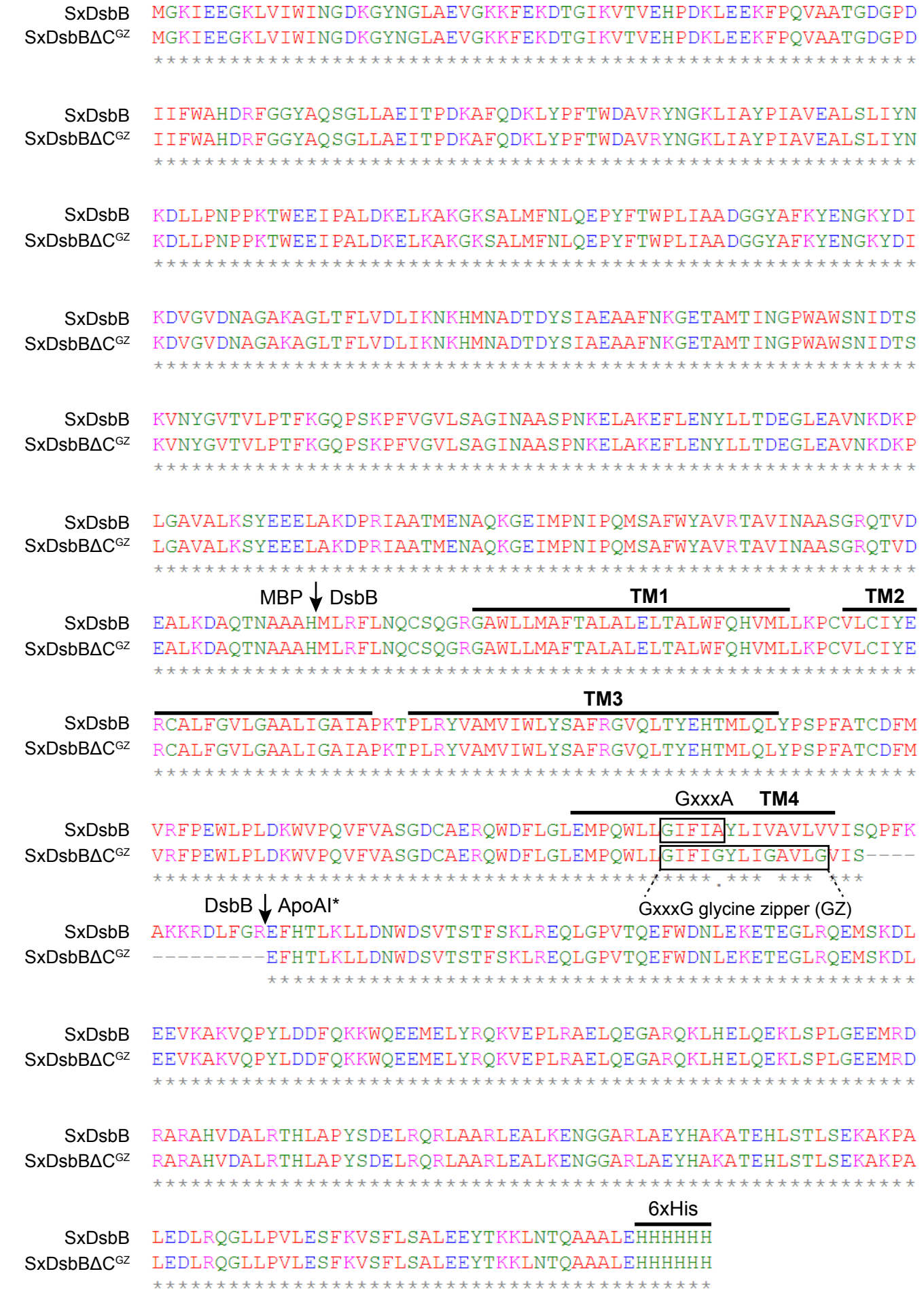

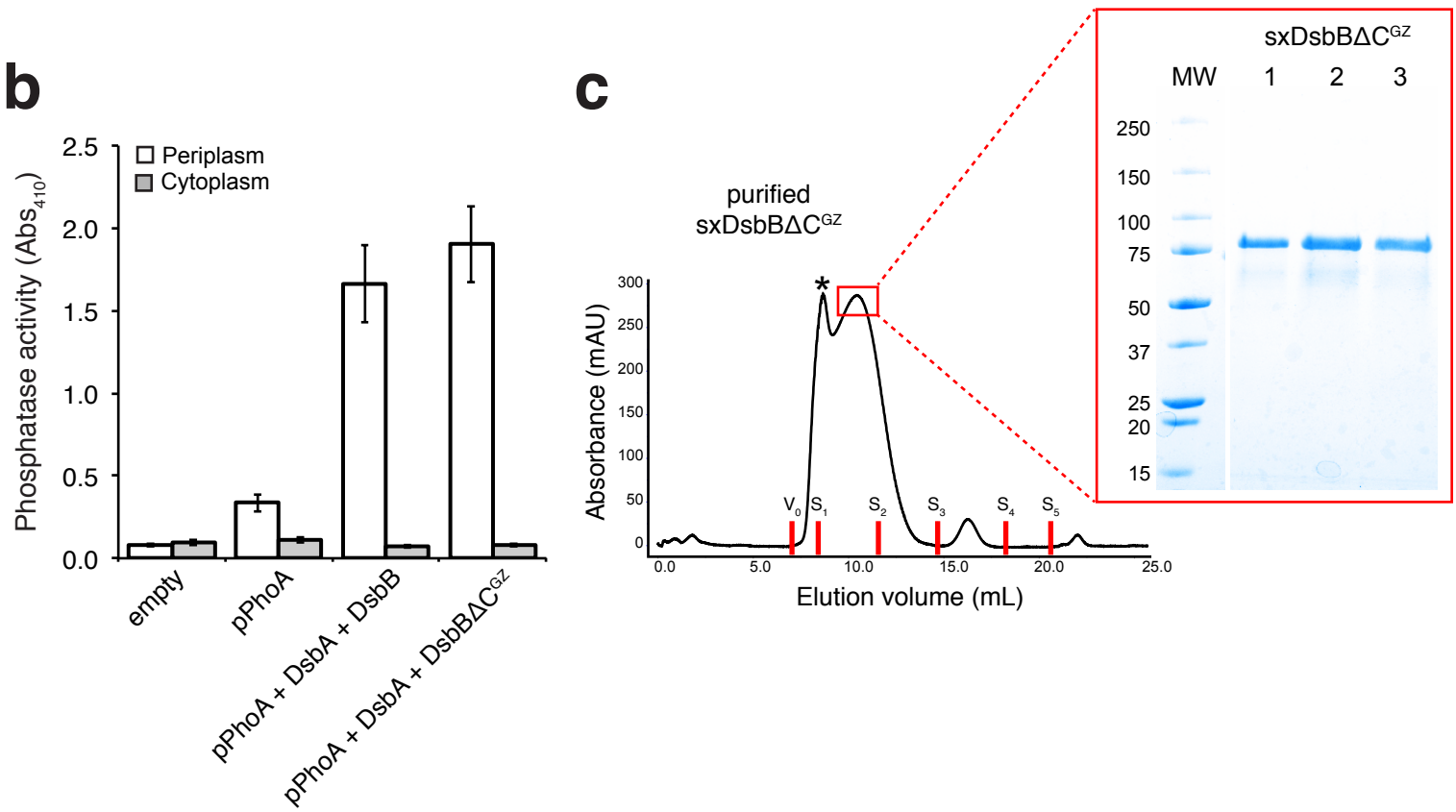

Supplementary Figure 1. Characterization of engineered sxDsbBΔC^{GZ} variant. (a) Primary sequence analysis and alignment (Clustal Omega, EMBL-EBI) of *E. coli* DsbB (accession number WP_000943457.1) and the engineered DsbBΔC^{GZ}. Black lines identify the transmembrane domains (TM). TM4 of wt DsbB contains a single GxxxA motif. An engineered concatenated GxxxA motif known as a glycine zipper (GZ) was seeded starting with the identified GxxxA motif in TM4. A C-terminal truncation was generated to eliminate excessive flexibility between DsbB and ApoAI* and potentially enhance solubility and stability. (b) Alkaline phosphatase activity measured in periplasmic (white bars) and cytoplasmic (gray bars) fractions derived from DHB4(DE3) Δ*dsbAB* cells carrying no plasmid (empty) or pBAD18-pPhoA (pPhoA), along with pET39b containing native DsbA and a pET21d derivative containing native DsbB or DsbBΔC^{GZ}. Data is the mean of biological triplicates and the error bars represent the standard error of the mean (SEM). (c) Size exclusion chromatography and Coomassie staining of SDS-PAGE gel (red box) of amylose affinity-purified sxDsbBΔC^{GZ}. The retention time (~10 mL) corresponds to a tetrameric form of sxDsbBΔC^{GZ}. The asterisk represents a soluble aggregate. A BioRad gel filtration standard was used to estimate the molecular weight of the eluted species and is marked in the panel as follows: V_0, column void volume; S_1, thyroglobulin (bovine) 670 kDa; S_2, γ-globulin (bovine) 158 kDa; S_3, ovalbumin (chicken) 44 kDa; S_4, myoglobin (horse) 17 kDa; and S_5, vitamin B12 1.4 kDa.

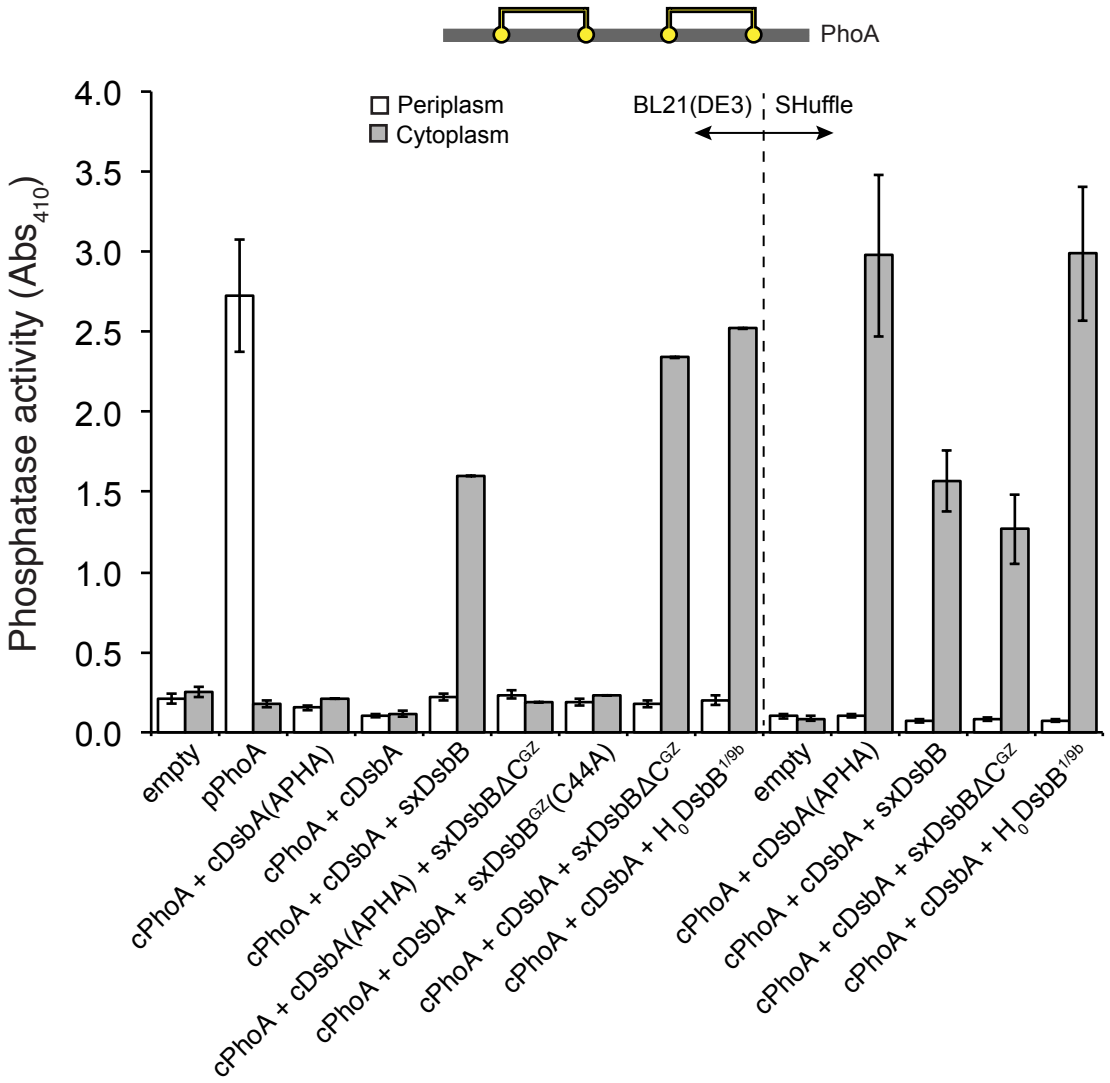

Supplementary Figure 2. Functional transfer of recompartmentalized pathway to other *E. coli* strains. Schematic shows disulfide bond connectivity for *E. coli* PhoA (2 disulfide bonds depicted by yellow circles connected by yellow lines). Alkaline phosphatase activity measured in periplasmic (white bars) and cytoplasmic (gray bars) fractions derived from: wt BL21(DE3) cells carrying no plasmid (empty), pBAD18-pPhoA (pPhoA), pFH273 (cPhoA + cDsbA), or pFH273mut (cPhoA + cDsbA(APHA)), along with a pET21d derivative containing SxDsbB, SxDsbBΔC^{GZ}, or H_0DsbB$^{1/9b}$ as indicated; and SHuffle cells carrying no plasmid (empty), pFH273 (cPhoA + cDsbA), or pFH273mut (cPhoA + cDsbA(APHA)), along with a pET21d derivative containing SxDsbB, SxDsbBΔC^{GZ}, or H_0DsbB$^{1/9b}$ as indicated. Data is the mean of biological triplicates and the error bars represent the standard error of the mean (SEM).

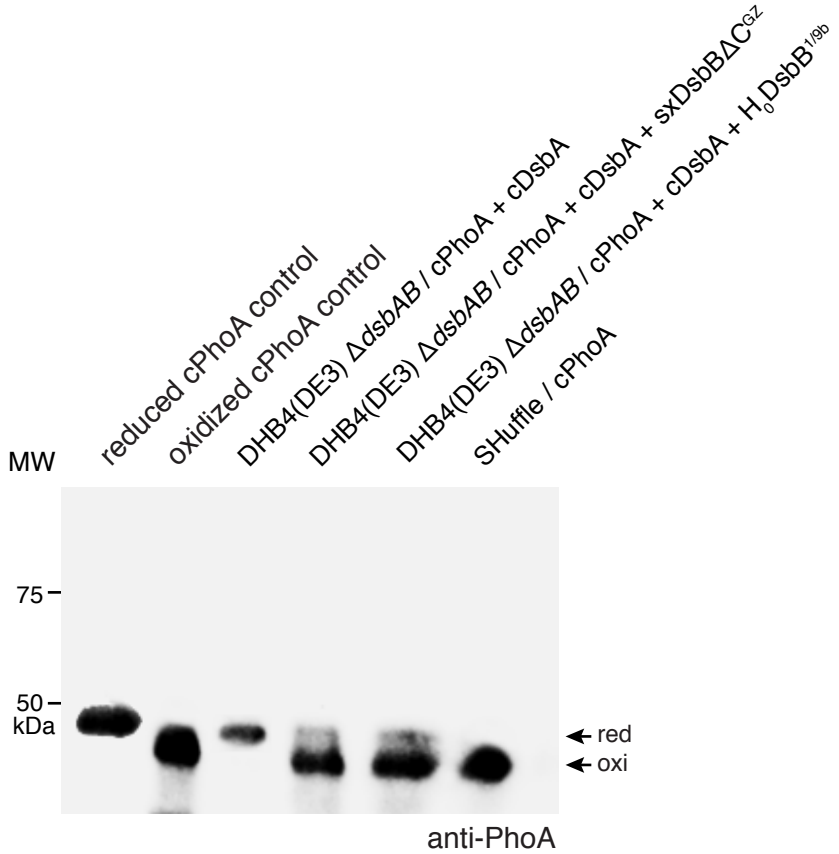

Supplementary Figure 3. Redox state of cPhoA. Redox state of AMS-alkylated cPhoA analyzed by Western blot using anti-PhoA antibody. Redox states of cPhoA are indicated as either reduced (red) or oxidized (oxi). Oxidized and reduced cPhoA control samples (lanes 1 and 2) were prepared by producing cPhoA in DHB4(DE3) Δ*dsbAB* cells and treating the protein with 4-DPS for oxidation or DTT for reduction prior to AMS alkylation. *In vivo* redox state of cPhoA was assayed in samples prepared from the strains as indicated (lanes 3-6). Molecular weight (MW) markers are shown on the left. Importantly, the blot pictured here was not cropped at the bottom. Rather, to ensure sufficient separation of the reduced and oxidized cPhoA species, gels were run at 200 mV for 40 min or until the 25-kDa band of the marker exited the gel. The blot presented here is representative of all three biological replicates.

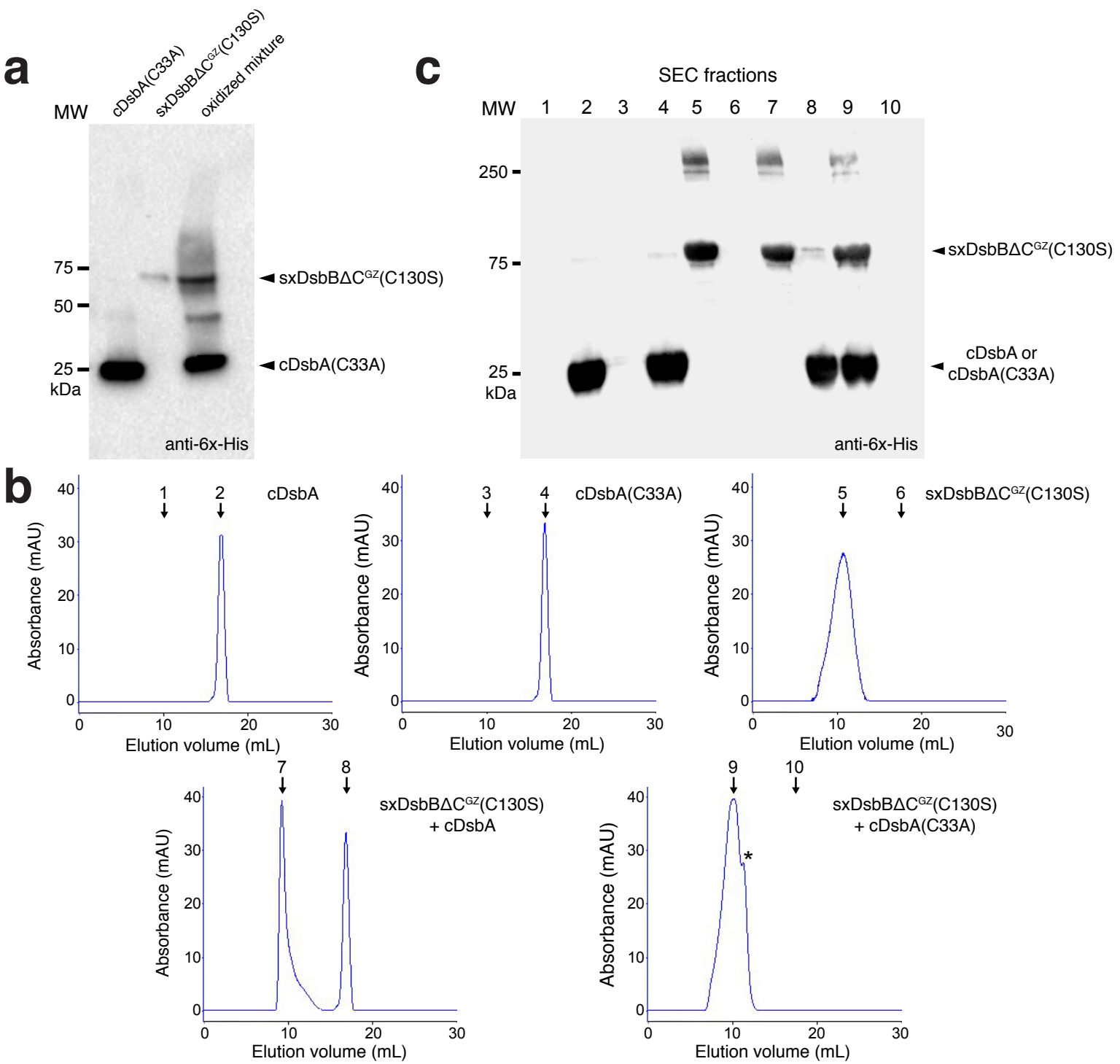

Supplementary Figure 4. Complex formation between sxDsbBΔC^{GZ}(C130S) and cDsbA(C33A). (a) Western blot analysis of cDsbA(C33A), sxDsbBΔC^{GZ}(C130S), and crosslinked sxDsbBΔC^{GZ}(C130S)-cDsbA(C33A). The cDsbA(C33A) and sxDsbBΔC^{GZ}(C130S) were individually expressed and purified. An oxidized mixture of the two constructs was then passed over amylose resin, washed extensively, and blotted using anti-6x-His antibody. The sxDsbBΔC^{GZ}(C130S) construct contains two tags, a C-terminal 6x-his tag and an N-terminal cMBP domain that binds to the amylose resin. Detection of cDsbA(C33A), that only contains a C-terminal 6x-His tag, in the oxidized mixture is thus due to crosslinking with sxDsbBΔC^{GZ}(C130S). (b) SEC chromatograms of all individual proteins (top panels) including wt cDsbA, cDsbA(C33A), and sxDsbBΔC^{GZ}(C130S), as well as oxidized mixtures of sxDsbBΔC^{GZ}(C130S) with either wt cDsbA or cDsbA(C33A) (bottom panels). It should be noted that NiNTA-purified DsbA(C33A) displayed two peaks in size exclusion, a monomer and a dimer. Both states of the DsbA(C33A) mutant have been previously reported and characterized structurally (Ondo-Mbele et al., *J Mol Biol* 2005). Only the monomer was employed in the downstream crosslinking for consistency. The typical retention volume for wt cDsbA (monomer) and monomeric cDsbA(C33A) was 17 mL. The retention volume for sxDsbBΔC^{GZ}(C130S) was 10 mL. An oxidized mixture of SxDsbBΔC^{GZ}(C130S) and wt cDsbA showed little to no evidence of interaction, as the two proteins eluted separately at their characteristic elution volumes. This lack of interaction was consistent with the short-lived nature of the complex formed between wt versions of DsbA and/or DsbB (Inaba et al. *Cell* 2006). In contrast, an interaction was clearly observed for the oxidized mixture of SxDsbBΔC^{GZ}(C130S) and monomeric cDsbA(C33A), as the proteins co-eluted in the early fraction, with no material eluting in the later fraction. Due to the resolution of the SEC column (Sepharose 200 10/300 GL) it was not possible to obtain a larger shift for the elution volume of the crosslinked product of sxDsbBΔC^{GZ}(C130S) + cDsbA(C33A). The asterisk corresponds to a shoulder that represents a small fraction of un-crosslinked sxDsbBΔC^{GZ}(C130S). (c) Western blot analysis of numbered SEC fractions (1-10) from (b). Odd and even numbers correspond to retention volumes of 10 mL and 17 mL, respetively. Blots were probed with anti-6x-His antibody.

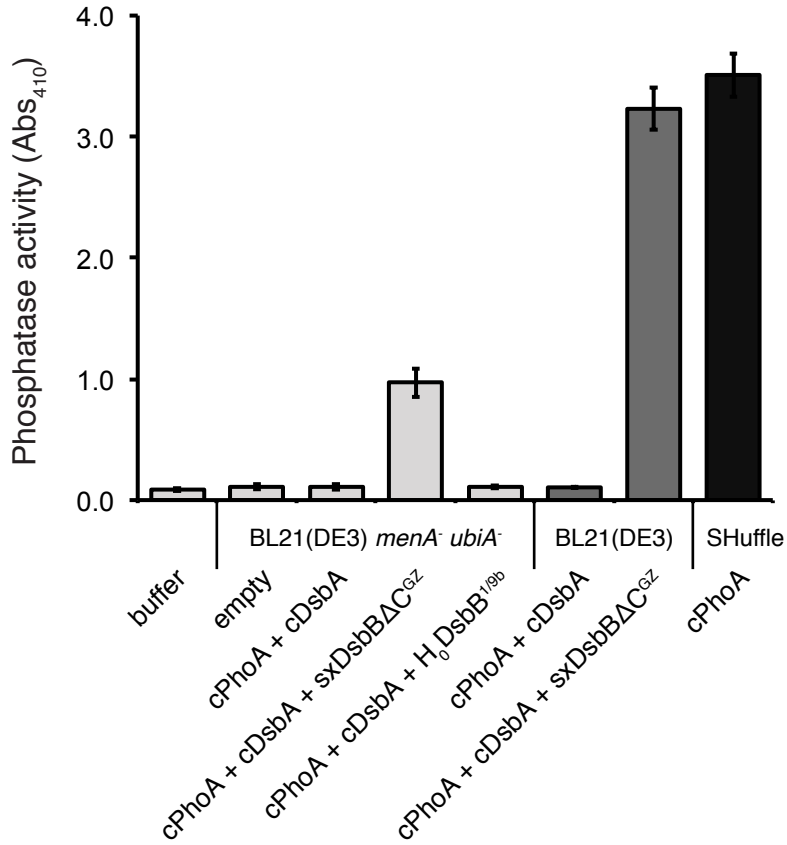

Supplementary Figure 5. cPhoA activation in a quinone-deficient strain background. Alkaline phosphatase activity measured in cytoplasmic fractions derived from BL21(DE3) Δ*menA* Δ*malF::kan…ubiA420* (BL21(DE3) *menA*$^-$ *ubiA*$^-$; light gray bars), BL21(DE3) (dark gray bars), or SHuffle (black bar), carrying the plasmids as indicated. For experiments performed using BL21(DE3) *menA*$^-$ *ubiA*$^-$ cells, 1 mM quinone precursor hydroxybenzoic acid (HBA) was supplemented to the culture as per Hatahet et al. (*J Mol Biol* 2013). Data is the mean of biological triplicates and the error bars represent the standard error of the mean (SEM).

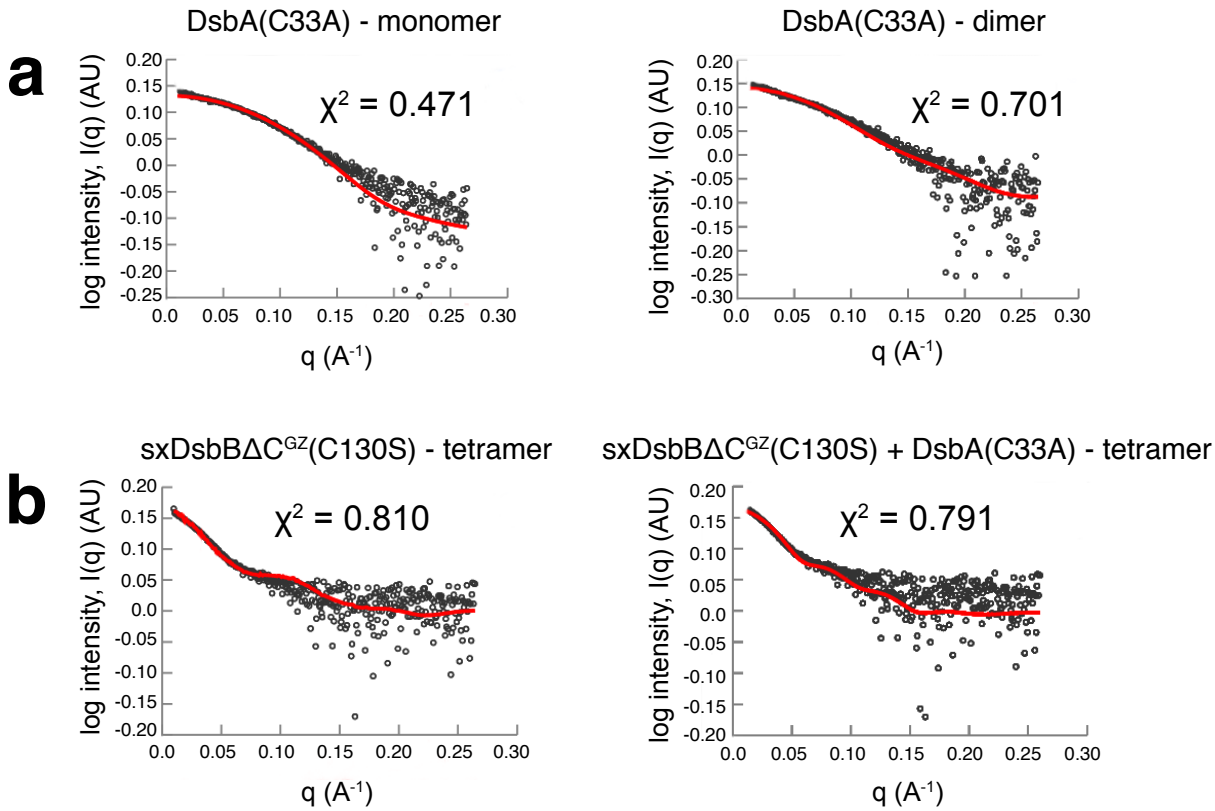

Supplementary Figure 6. Structural characterization of SxDsbBΔC^{GZ} by biological SAXS. The mathematical representation of the fit for the corresponding crystal structure and its calculated envelope (log intensity, I(q), versus q) is plotted for each of the following constructs: (a) cDsbA(C33A) as a monomer (left) or dimer (right) and (b) tetrameric SxDsbBΔC^{GZ}(C130S) (left) and tetrameric SxDsbBΔC^{GZ}(C130S) crosslinked to cDsbA(C33A) (right). Goodness of fit was assessed by a chi-squared (χ^2) test. Small χ^2 values indicate that the calculated SAXS curve agrees with the experimental data within error. Black circles are the experimental values and the red line is the profile of the theoretical model.

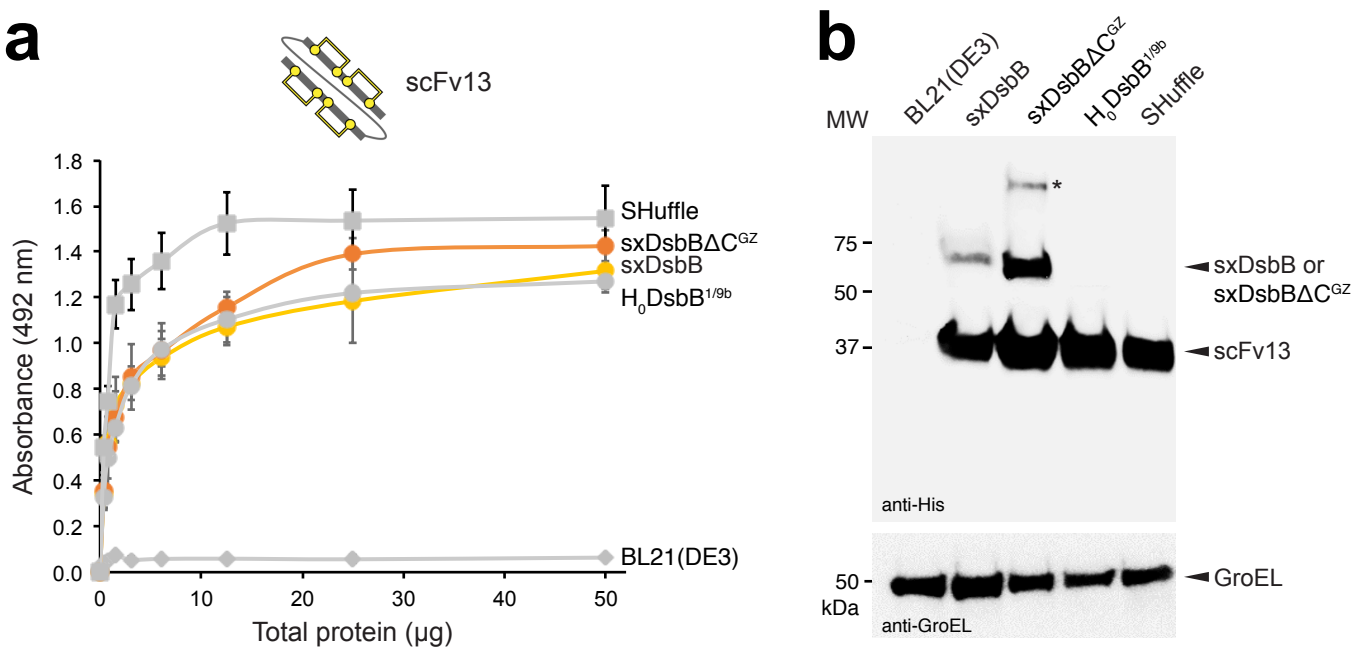

Supplementary Figure 7. Folding of antibody fragments by solubilized DsbB variants. (a) Schematic shows disulfide bond connectivity for antibody fragment scFv13 (4 disulfide bonds depicted by yellow circles connected by yellow lines), which is specific for *E. coli* β-gal. ELISA signals (Abs_{492}) for soluble lysates derived from BL21(DE3) or SHuffle cells carrying plasmid(s) for expressing the different constructs as indicated. ELISA plates were coated with β-gal as antigen. The activity measured in BL21(DE3) cells carrying only the scFv13-encoding plasmid served as a negative control. Data is expressed as the mean ± standard error of the mean (SEM) of biological triplicates. (b) Western blot analysis of same soluble lysates assayed in (a). Blots were probed with anti-6x-His antibody to detect scFv13 (top panel) and anti-GroEL antibody to detect GroEL (bottom panel), which served as a cytoplasmic fractionation marker and loading control. Note that the 6x-His-tagged sxDsbB and sxDsbBΔC^{GZ} proteins were also detected, as well as an oligomeric form of sxDsbBΔC^{GZ} (possibly a tetramer) at higher molecular weights. Topologically inverted DsbB was also 6x-His-tagged but was not detected when soluble extracts were prepared (see also Figure 2). Molecular weight (MW) markers are shown on the left.

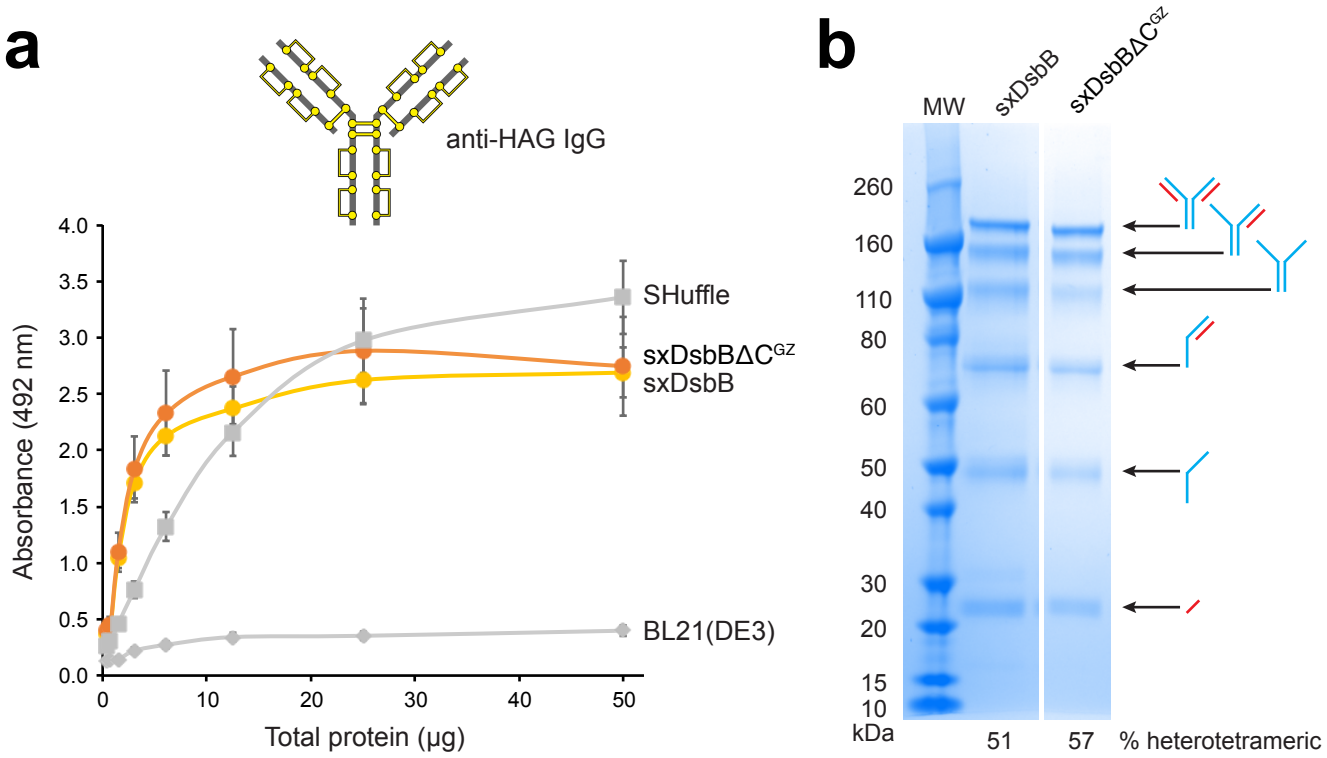

Supplementary Figure 8. Folding and assembly of full-length antibodies by solubilized DsbB variants. (a) Schematic shows disulfide bond connectivity for anti-HAG cyclonal IgG (16 disulfide bonds depicted by yellow circles connected by yellow lines), which is specific for influenza virus hemagglutinin (HAG). ELISA signals (Abs_{492}) for soluble lysates derived from BL21(DE3) or SHuffle cells carrying plasmid(s) for expressing the different constructs as indicated. ELISA plates were coated with GST-HAG as antigen. The activity measured in BL21(DE3) cells carrying only the anti-HAG cyclonal IgG plasmid served as a negative control. Under the conditions tested here, it was impossible to obtain reproducible results using $H_0DsbB^{1/9b}$. Data is expressed as the mean ± standard error of the mean (SEM) of biological triplicates. (b) Cooomassie-stained SDS-PAGE gel of anti-HAG cyclonal IgGs purified from soluble lysates in (a) using Protein A affinity chromatography. Arrows indicate fully assembled cyclonal as well as other intermediate species. The percentage of fully assembled heterotetrameric product among all product was 51 and 57% for sxDsbB and sxDsbBΔC^{GZ}, respectively, as determined by densitometry analysis. Molecular weight (MW) markers are shown on the left.

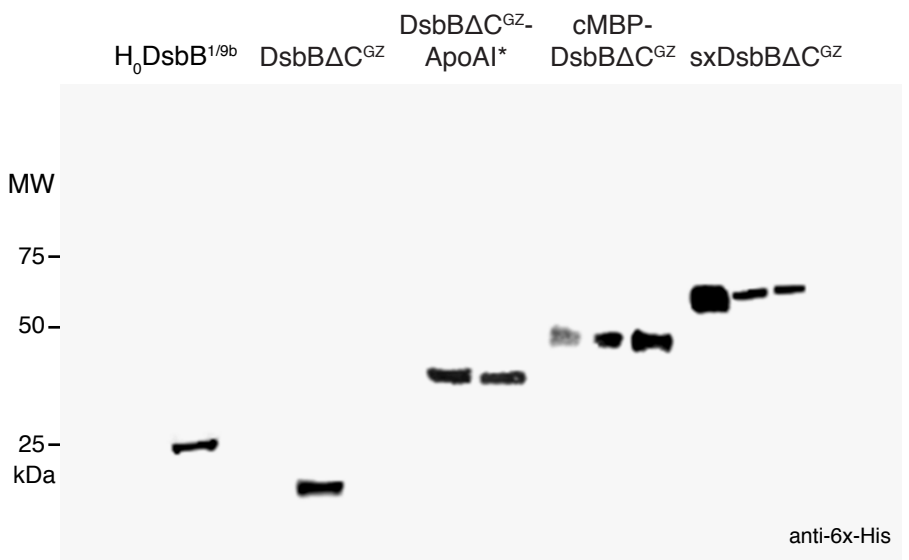

Supplementary Figure 9. Uncropped images of Figure 2 immunoblots.

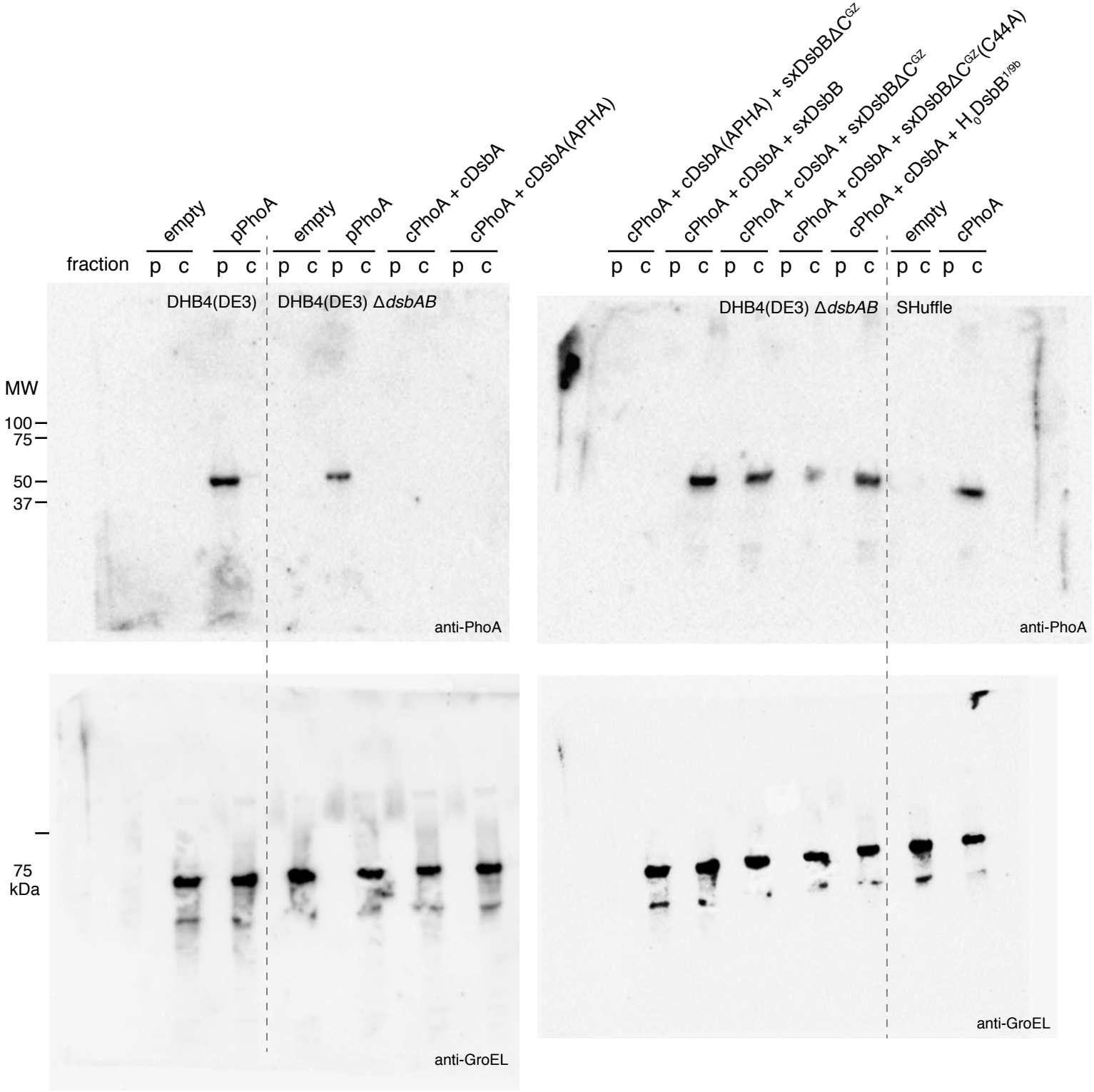

Supplementary Figure 10. Uncropped images of Figure 3 immunoblots.

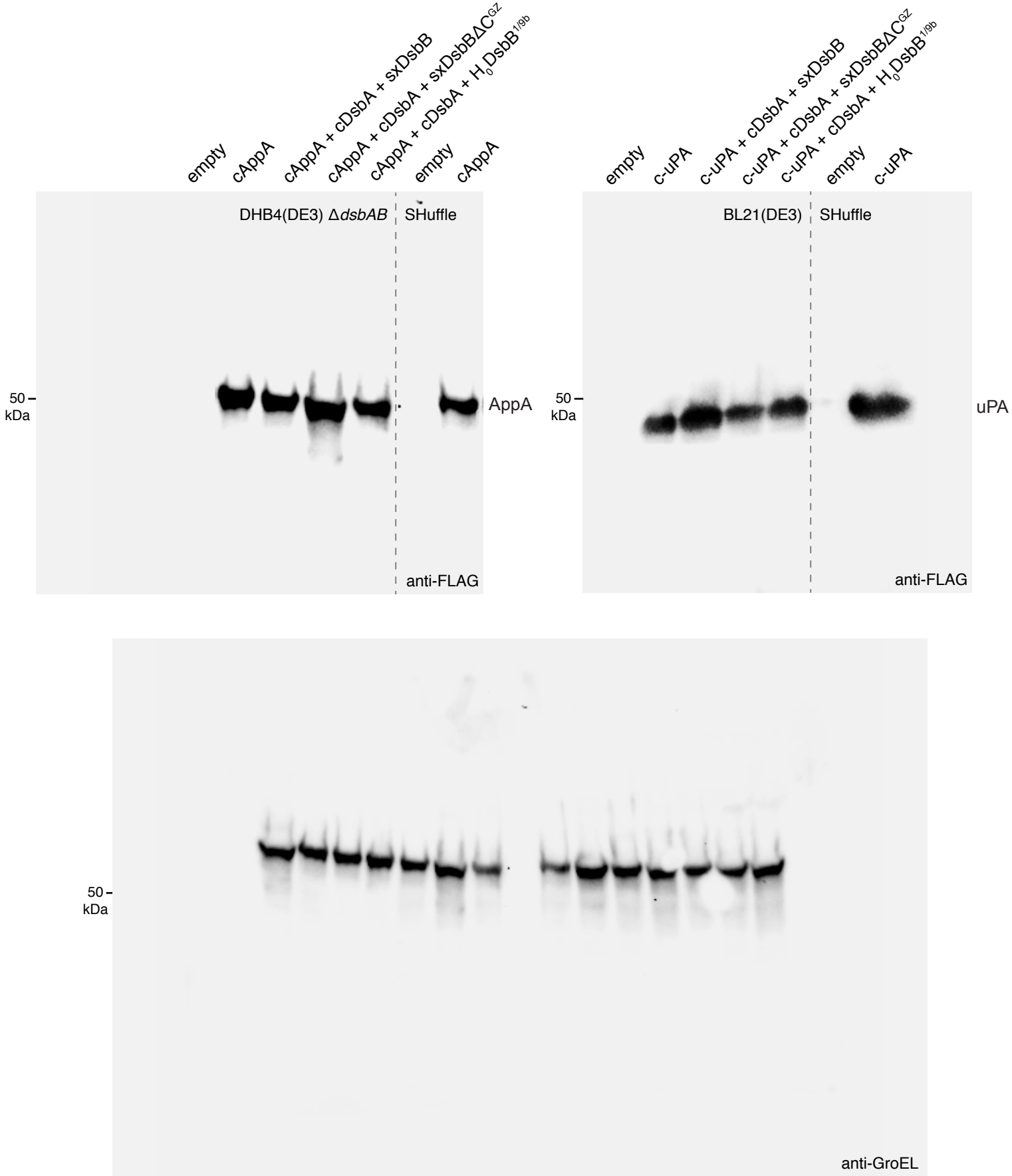

Supplementary Figure 11. Uncropped images of Figure 5 immunoblots.

Supplementary Table 1. Plasmids used in this study

Name	Description	Reference
pCP20	Temperature-sensitive replication and thermal induction of FLP synthesis; Amp^R, Cm^R	[1]
pET-GFP	Gene encoding green fluorescent protein cloned in pET21a; Amp^R	[2]
pBAD18-Cm	Plasmid containing the arabinose P_{BAD} promoter; Cm^R	[5]
pBAD-pPhoA	Gene encoding full-length *E. coli* alkaline phosphatase (PhoA) cloned in pBAD18-Cm; Cm^R	This study
pFH265	Gene encoding topologically inverted DsbB variant $H_0DsbB^{1/9b}$ cloned in pET23; Amp^R	[3]
pFH277	Plasmid pLysS backbone cloned into pBAD/*araC* resulting in hybrid plasmid pLysSBAD; Cm^R	[3, 4]
pFH273	Bicistronic expression of genes encoding cPhoA (R22-K471) and 6x-His-cDsbA (A20-K208) cloned in plasmid pLysSBAD; Cm^R	[3]
pFH-cPhoA	As plasmid pFH273 but with gene encoding 6x-His-cDsbA removed; Cm^R	This study
pFH273mut	As plasmid pFH273 but with gene encoding inactive cDsbA(APHA) mutant; Cm^R	This study
pET24-cPhoA	Gene encoding cPhoA (R22-K471) cloned in pET24b; Cm^R	This study
pET28-ΔspMBP-DsbB-ApoAI*	Chimeric gene comprised of *E. coli* MBP lacking its signal peptide (K27-T395); ΔspMBP or cMBP), *E. coli* DsbB, and truncated human ApoAI (Δ1-43; ApoAI*) cloned in pET28a; Kan^R	[7]
pET21-sxDsbB	Chimeric cMBP-DsbB-ApoAI* cloned from pET28-ΔspMBP-DsbB-ApoAI* into pET21d; Amp^R	This study
pET21-sxDsbBΔC^{GZ}	As pET21-sxDsbB but with truncated DsbB (M1-S163) and A152G, V156G, V160G mutations in DsbB; Amp^R	This study
pET21-sxDsbBΔC^{GZ}(C44A)	As pET21-sxDsbBΔC^{GZ} but with additional C44A mutation in DsbB; Amp^R	This study
pET21-sxDsbBΔC^{GZ}(C130S)	As pET21-sxDsbBΔC^{GZ} but with additional C130S mutation in DsbB; Amp^R	This study
pET21-DsbB	As pET21-sxDsbB but without genes encoding cMBP and ApoAI*; Amp^R	This study
pET21-DsbBΔC^{GZ}	As pET21-sxDsbBΔC^{GZ} but without genes encoding cMBP and ApoAI*; Amp^R	This study
pET21-cMBP-DsbB	As pET21-sxDsbB but without gene encoding ApoAI*; Amp^R	This study
pET21-cMBP-DsbBΔC^{GZ}	As pET21-sxDsbBΔC^{GZ} but without gene encoding ApoAI*; Amp^R	This study
pET21-DsbB-ApoAI*	As pET21-sxDsbB but without gene encoding cMBP; Amp^R	This study
pET21-DsbBΔC^{GZ}-ApoAI*	As pET21-sxDsbBΔC^{GZ} but without gene encoding cMBP; Amp^R	This study
pET39b	Gene encoding *E. coli* DsbA in pET backbone; Kan^R	Novagen
pET39b-C33A	As pET39b but with C33A mutation in DsbA; Kan^R	This study
pET28-BicExp	Bicistronic expression plasmid derived from pET28a; Kan^R	Lab stock
pET28-sxDsbB::GST-cDsbA	Bicistronic expression of genes encoding sxDsbB and GST-cDsbA from pET28a; Kan^R	This study
pET28-sxDsbBΔC^{GZ}::GST-cDsbA	As pET28-sxDsbB-GST-cDsbA but with sxDsbBΔC^{GZ}; Kan^R	This study
pET28- sxDsbBΔC^{GZ}::GST-cDsbA(APHA)	As pET28-sxDsbBΔC^{GZ}::GST-cDsbA but with gene encoding inactive cDsbA(APHA); Kan^R	This study

pET28-sxDsbBΔC^{GZ}(C44A)::GST-cDsbA	As pET28-sxDsbBΔC^{GZ}::GST-cDsbA but with gene encoding inactive sxDsbBΔC^{GZ}(C44A); Kan^{R}	This study
pET28-H$_0$DsbB$^{1/9b}$::GST-cDsbA	As pET28-sxDsbB-GST-cDsbA but with H$_0$DsbB$^{1/9b}$; Kan^{R}	This study
pHIS.parallel1	Hybrid T7 promoter-based plasmid created by combining pFastBac-HTa and pET22b; Amp^{R}	[8]
pHIS-cAppA	Gene encoding *E. coli* AppA lacking its N-terminal signal peptide and modified with N-terminal 6x-His tag in pHIS.parallel1; Amp^{R}	This study
pET24b-urokinase-HIS	Gene encoding cytoplasmic murine urokinase (c-uPA) cloned in pET24b; Cm^{R}	[6]
pTrc99A-scFv13	Gene encoding single-chain Fv antibody fragment against *E. coli* β-gal cloned in pTrc99A; Amp^{R}	[9]
pET21b-cyclonal-HAG(mFab/hFc)	Genes encoding heavy and light chains of anti-HAG cyclonal IgG with murine Fab (mFab) and human Fc (hFc) cloned in pET21b; Amp^{R}	[10]

References

1. Cherepanov, P.P. and W. Wackernagel, *Gene disruption in Escherichia coli: TcR and KmR cassettes with the option of Flp-catalyzed excision of the antibiotic-resistance determinant.* Gene, 1995. **158**(1): p. 9-14.
2. Contreras-Martinez, L.M., J.T. Boock, J.S. Kostecki, and M.P. DeLisa, *The ribosomal exit tunnel as a target for optimizing protein expression in Escherichia coli.* Biotechnol J, 2012. **7**(3): p. 354-60.
3. Hatahet, F. and L.W. Ruddock, *Topological plasticity of enzymes involved in disulfide bond formation allows catalysis in either the periplasm or the cytoplasm.* J Mol Biol, 2013. **425**(18): p. 3268-76.
4. Hatahet, F., V.D. Nguyen, K.E. Salo, and L.W. Ruddock, *Disruption of reducing pathways is not essential for efficient disulfide bond formation in the cytoplasm of E. coli.* Microb Cell Fact, 2010. **9**: p. 67.
5. Guzman, L.M., D. Belin, M.J. Carson, and J. Beckwith, *Tight regulation, modulation, and high-level expression by vectors containing the arabinose PBAD promoter.* J Bacteriol, 1995. **177**(14): p. 4121-30.
6. Lobstein, J., C.A. Emrich, C. Jeans, M. Faulkner, P. Riggs, and M. Berkmen, *SHuffle, a novel Escherichia coli protein expression strain capable of correctly folding disulfide bonded proteins in its cytoplasm.* Microb Cell Fact, 2012. **11**: p. 56.
7. Mizrachi, D., Y. Chen, J. Liu, H.M. Peng, A. Ke, L. Pollack, R.J. Turner, R.J. Auchus, and M.P. DeLisa, *Making water-soluble integral membrane proteins in vivo using an amphipathic protein fusion strategy.* Nat Commun, 2015. **6**: p. 6826.
8. Sheffield, P., S. Garrard, and Z. Derewenda, *Overcoming expression and purification problems of RhoGDI using a family of "parallel" expression vectors.* Protein Expr Purif, 1999. **15**(1): p. 34-9.
9. Contreras-Martinez, L.M. and M.P. DeLisa, *Intracellular ribosome display via SecM translation arrest as a selection for antibodies with enhanced cytosolic stability.* J Mol Biol, 2007. **372**(2): p. 513-24.
10. Robinson, M.P., N. Ke, J. Lobstein, C. Peterson, A. Szkodny, T.J. Mansell, C. Tuckey, P.D. Riggs, P.A. Colussi, C.J. Noren, C.H. Taron, M.P. DeLisa, and M. Berkmen, *Efficient expression of full-length antibodies in the cytoplasm of engineered bacteria.* Nat Commun, 2015. **6**: p. 8072.